Progress in Aerospace Sciences 63 (2013) 56–66

Contents lists available at ScienceDirect

Progress in Aerospace Sciences

journal homepage: www.elsevier.com/locate/paerosci

An overview of the autonomous navigation for a gravity-assist interplanetary spacecraft

Xin Ma *, Jiancheng Fang, Xiaolin Ning

School of Instrumentation Science and Opto-electronics Engineering, Beihang University, Beijing 100191, China

ARTICLE INFO

Available online 2 August 2013

Keywords:
Deep space exploration
Gravity assist
Autonomous navigation
Navigation system

ABSTRACT

Gravity assist technique plays an important role in deep space missions so that the interplanetary spacecraft can travel to further space with lower energy. A gravity-assist orbit demands accurate navigation in the approach period, helping the explorer achieve orbit insertion and change velocity accurately. The conventional Doppler-Range radio navigation method can hardly satisfy the gravity-assist deep space mission requirement of high performance in accuracy, real time and coverage, while autonomous navigation technology can guarantee the success of gravity assist mission. In this article the principle and mechanics of gravity assist and autonomous navigation is summarized, and the survey of autonomous navigation technology in deep space mission is provided and analyzed. The key technology and the development trends of autonomous navigation are also put forward. The comprehensive analyses can provide reference for development of autonomous navigation technology for spacecraft using gravity assist.

Contents

* Corresponding author. Tel.: +86 10 82 338 820; fax: +86 10 823 168 13.
E-mail address: maxin@aspe.buaa.edu.cn (X. Ma).

0376-0421/$ - see front matter © 2013 Elsevier Ltd. All rights reserved.
http://dx.doi.org/10.1016/j.paerosci.2013.06.003

1. Introduction

In the 21st century, deep space explorations move into a new era. U.S, Europe, Russia, Japan, India, and China have made a tight and long-term schedule of deep space explorations. Planets, natural satellites are planned to be explored by a manned mission or a robotic and unmanned mission, which can lead us, human being, to the deep space 380 thousand kilometers away. Since 2007, China has successfully launched two lunar orbiters: Chang'e-1 (CE-1) and Chang'e-2 (CE-2). In the future a soft-lander, a rover, and an automated sample return spacecraft will be launched in phases II and III of the Chinese Lunar Exploration Program. The experience of Lunar Exploration Program will enhance the confidence and capability for future deep space explorations of China. In addition, with the help of the advanced technologies and the prosperous economy, China has the capability of exploring Mars and even the other planets in the solar system. Therefore, explorations of the Sun, Mars, Venus, and asteroids, etc. are expected in the future [1–4].

With the rapid expansion of deep space exploration of the solar system, the velocity increment required for a direct ballistic transfer increases significantly, which is the major obstacle of deep space missions. Fortunately, gravity-assist (GA) technologies can help a spacecraft reduce the propulsive requirements to travel between the planets, which are widely used in interplanetary missions. Gravity assist is described as the effect when the spacecraft enters a planetary sphere of influence and gains or loses energy with respect to the sun. The energy change is caused by the rotation of the spacecraft's velocity vector under the influence of the secondary planet's gravitational field, which results in a change in the direction and magnitude of the heliocentric velocity of the spacecraft [5,6].

Although the use of Gravity Assist reduces the propulsion requirement of space missions, the navigation system for a gravity-assist mission faces more challenge to keep the spacecraft flying the designed tour accurately and punctually. Position and time are tightly restricted in obtaining proper energy from the gravity-assist planet. Accordingly, the accuracy requirement for gravity assist is as strict as that of a planet encounter.

To ensure the success of a gravity-assist mission, the navigation system must be configured appropriately. Two major navigation methods, ground-based navigation and autonomous navigation, are used to meet the strict navigation requirement of gravity assist. The accuracy of ground-based navigation is heavily dependent on the knowledge of the ephemeris of the target celestial body. Additionally, ground-based navigation is not a real-time process owing to the long signal delay caused by the enormous distance between the spacecraft and the Earth. As a result, an autonomous navigation system becomes a fundamental configuration for a successful gravity-assist mission because of the excellent relative navigation accuracy and real-time performance.

The paper is separated into several sections: after the introduction, principles of the autonomous navigation in cruise and approach phases are described in Section 2. Section 3 provides a survey of the successful applications of the autonomous navigation technology in gravity-assist interplanetary missions. In Section 4, key-point technologies supporting the accurate navigation for gravity-assist missions are analyzed and summarized. In Section 5, trends of autonomous navigation are presented. Finally, conclusions are drawn in Section 6.

2. Principle of autonomous navigation for a gravity-assist interplanetary spacecraft

2.1. B-plane

Autonomous navigation system provides results for orbit maneuver system, and the use of *B*-plane coordinate system is a convenient method for orbit insertion maneuver. The orbit parameters and their errors can be described in *b*-plane, and the correct maneuvers are designed and implemented to achieve the precise orbit insertion by the comparison between the estimated orbit parameters and nominal parameters. Therefore the navigation parameters for interplanetary missions are usually described in the b-plane coordinate system. The definition of the *b*-plane is shown in Fig. 1 [7].

The *b*-plane coordinate system is centered on the target body and perpendicular to the hyperbolic excess velocity. In the *B*-plane, $\boldsymbol{S}$ is the vector of the incoming asymptote, which is parallel to the hyperbolic excess velocity $\boldsymbol{V}_{\infty,\mathrm{in}}$. $\boldsymbol{B}$ is the target vector which passes through the target body and is perpendicular to the incoming asymptote $\boldsymbol{S}$. The unit vectors, $\boldsymbol{T}$ and $\boldsymbol{R}$, lie in the *b*-plane as axes. $\boldsymbol{T}$ is a unit vector normal to $\boldsymbol{S}$ and parallel to the ecliptic plane. $\boldsymbol{R}$ is a unit vector to form a right-handed system [8,9]. The spacecraft achieves the initial $\boldsymbol{B}\cdot\boldsymbol{R}$ and $\boldsymbol{B}\cdot\boldsymbol{T}$ of the reference trajectory by orbital maneuver, which allows velocity being in accordance with the nominal velocity when the spacecraft departs the sphere of influence of the assisted-planet, and targeting during a gravity assist. The *b*-plane uncertainty elliptical area represents uncertainty in the predicted trajectory of the spacecraft.

2.2. Principle of the autonomous navigation during the cruise phase

The basic idea of autonomous navigation during cruise phase is shown in Fig. 2. Considering celestial bodies (asteroid and planets) as beacons, a single sighting of a beacon places the spacecraft along

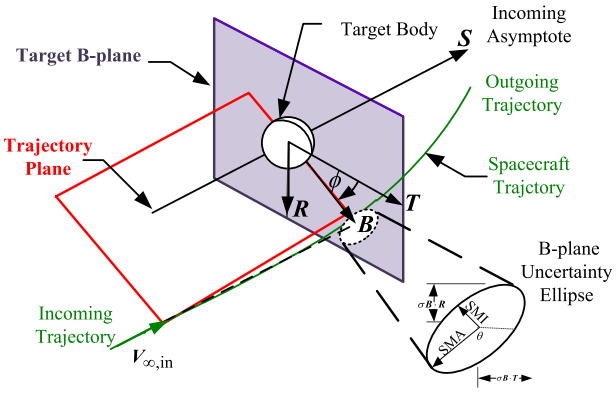

Fig. 1. The *b*-plane coordinate system.

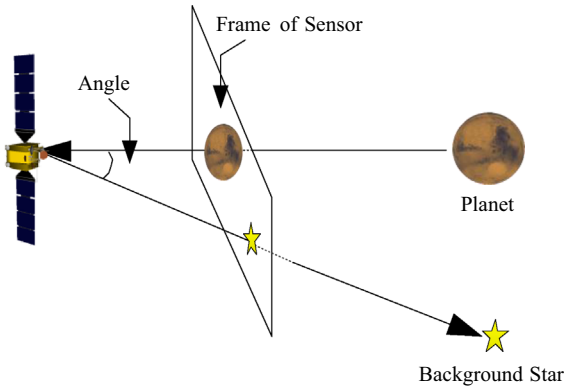

Fig. 3. Angle between star and planet.

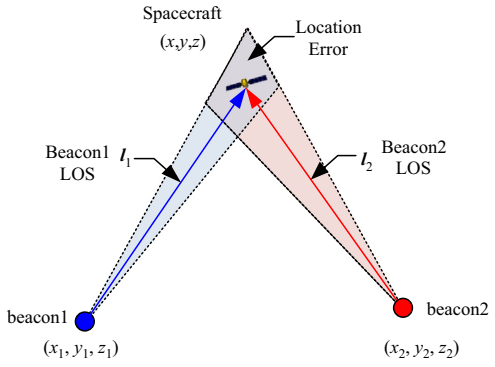

Fig. 2. The principle of autonomous navigation during cruise phase.

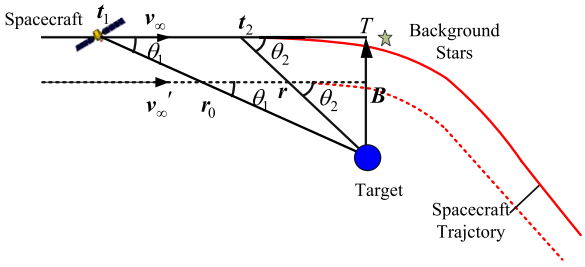

Fig. 4. The principle of autonomous navigation during approach phase.

the line of sight (LOS), and at least two LOS values can determine the position of the spacecraft [10,11]. The two LOS values of beacons are measured from the pictures of beacons against the background stars captured by the on-board camera. With the known ephemerides of beacons, the positions of the beacons in the pictures determinately fix their LOS. The coordinates of beacon1 and beacon2 in the heliocentric inertial system are (x_1, y_1, z_1) and (x_2, y_2, z_2). The LOS values of beacon1 and beacon2 measured in the inertial system are $\boldsymbol{l}_1 = (a_1, b_1, c_1)$ and $\boldsymbol{l}_2 = (a_2, b_2, c_2)$. The lines determined by $\boldsymbol{l}_1$ and $\boldsymbol{l}_2$ can be expressed as follows:

$$\begin{cases} \frac{x-x_1}{a_1} = \frac{y-y_1}{b_1} = \frac{z-z_1}{c_1} \\ \frac{x-x_2}{a_2} = \frac{y-y_2}{b_2} = \frac{z-z_2}{c_2} \end{cases} \tag{1}$$

Therefore, the point of intersection, the spacecraft coordinates (x, y, z), can be obtained from Eq. (1).

The determination process of the heliocentric inertial vector $\boldsymbol{l}_1$ and $\boldsymbol{l}_2$ requires the pointing direction of the camera boresight, which can be provided by stars in the background. The stars are so distant that their position in the sky can be considered as a fixed point. After the camera takes the picture of stars, according to the pixels and lines of stars, the pointing direction can be derived from a least-squares filter. The navigation results mentioned above are described in heliocentric frame. After involving the frame transformations, the results are mapped into the planet *B*-plane [9].

2.3. Principle of autonomous navigation during the approach phase

During the approach phase, the number of the observable celestial body is limited. Only assisted-planet is able to be observed. Therefore with the assistance of the previous and current history of the LOS to the target body, the spacecraft position can be determined. The LOS to the target body and background stars can be obtained from the navigation camera, and the angles between background stars and planet are indirectly calculated (Fig. 3) [12].

The time of flight and *B*-plane parameter can be obtained by measuring the angles θ_1 and θ_2 between background stars and the assisted-planet at the times t_1 and t_2 (For simplicity the background star is assumed to lie along the v_∞ vector, the incoming asymptote direction.). Fig. 4 shows the time of flight T, the target vector $\boldsymbol{B}$, the hyperbolic exceed velocity v_∞, and their relationships.

$$\begin{cases} \tan\theta_1 = x/(T-t_1) \\ \tan\theta_2 = x/(T-t_2) \end{cases}, \quad x = \frac{B}{v_\infty} \tag{2}$$

Solving for x and time of fight T gives

$$x = \frac{(t_2-t_1)\tan\theta_1 \ \tan\theta_2}{\tan\theta_2 - \tan\theta_1} \tag{3}$$

$$T = \frac{t_1\tan\theta_1 - t_2\tan\theta_2}{\tan\theta_1 - \tan\theta_2} \tag{4}$$

However, in general only x can be obtained and discrimination between $\boldsymbol{B}$ and v_∞, as shown in Fig. 4. The observations, θ_1 and θ_2, are perfectly same for both trajectories (the full line and the dotted line) which are different in $\boldsymbol{B}$ and v_∞. There are two methods to recognize $\boldsymbol{B}$ and v_∞. One method is to combine radiometric data to obtain v_∞ very accurately. Another method is when spacecraft approaches the planet, parallax effects in the case of the natural satellite observations allow one to solve for v_∞, and the time of flight solution becomes less sensitive to pointing errors. Furthermore, the natural satellite's ephemeris will be estimated relative to the target planet to reduce ephemeris error effects [13,14].

3. A survey of autonomous navigation technology development

Gravity assist technique has been successfully applied in many interplanetary missions. Thirteen of seventeen gravity-assist interplanetary missions have an autonomous navigation system, which provides precision navigation information to the trajectory control system, and contributes gravity-assist success eventually.

3.1. Galileo

Galileo was launched on October 18, 1989, and arrived at Jupiter in December 1995, via gravity assist flybys of Venus, Earth, beginning the first scientific exploration of Jupiter and its satellite. On the way to Jupiter, the spacecraft had a close flyby of 951 Gaspra and 243 Ida, and discovered the first moon of Asteroid, Dactyl, around the asteroid 243 Ida. Galileo obtained Earth-based radio measurements and four optical navigation pictures of the Gaspra and stars by the Solid State Imaging (SSI), and Galileo successfully accomplished the encounter with the asteroid by 10 km navigation accuracy. Before the spacecraft encountered Jupiter, two-way S-band Doppler and optical pictures were used for navigation. The pictures of Jupiter, Galilean moons and background stars obtained by SSI provided accurate navigation for the spacecraft [15–18].

3.2. Hiten

The Hiten spacecraft, MUSES-A, was launched on January 24, 1990. After the tenth swing-by to the Moon and second aerobraking by the earth's atmosphere, Hiten had enough fuel to change into the circumlunar moon orbit. The optical navigation sensor is developed to detect the moon and background stars to determine the moon's direction in the inertial frame with an accuracy of better than 1′. Its optical navigation system is the world's first system for a spin-stabilizing satellite [19–22].

3.3. Near Earth Asteroid Rendezvous

Near Earth Asteroid Rendezvous (NEAR) was launched by the U.S. National Aeronautics and Space Administration (NASA) on February 17, 1996. The spacecraft made a successful close flyby of the asteroid 433 Eros, then went into orbit around Eros, and soft-landed on the asteroid finally. The spacecraft's trajectory took it to the asteroid 253 Mathilde, and then the spacecraft returned to Earth for a gravity assist to encounter Eros. Unlike a planetary orbiter, the very low gravity of the asteroid means the spacecraft can easily escape Eros or crash into its surface with little change in velocity. This places additional demand on navigation accuracy while also imposing a generally shorter response time than that usual for planetary orbit missions.

Navigation for NEAR uses radiometric and optical data types, and laser range is available when the spacecraft is below 100 km altitude. During the Earth Swingby, Multispectral Imager (MSI) observed both Earth and the Moon to test the performance. During the terminal approach to Eros, the navigation for NEAR relies on imaging a target body against a background of reference stars by MSI. Unlike planetary orbiter missions, navigation for NEAR depends on rapid estimates of non-gravitational accelerations and asteroid physical parameters, such as spin state, gravity field, shape, etc [23–25].

3.4. Cassini–Huygens

Cassini–Huygens, a joint undertaking between NASA, European Space Agency (ESA), and the Italian Space Agency (ASI), was launched on October 15, 1997, and at present its extended mission is still in progress. After an interplanetary voyage which included four flybys, two at Venus, one at Earth, and one at Jupiter, they entered into orbit around Saturn and its moon Titan. Two types of navigation observing data are available during the approach phase. One is radiometric data via NASA's Deep Space Network (DSN), including 2-way X-Band Doppler and range tracking data. Another is on-board optical navigation images of the major Saturn satellites against a background of stars acquired via the Narrow Angle Camera (NAC) of Imaging Science Subsystem (ISS). The positions of the planets in the measurement model are derived from DE410 Ephemeris. Pseudo-epoch state estimation filter is used to estimate the spacecraft epoch, state, the correction to the Saturn ephemeris, the satellite states, their mass, the Saturn pole, Saturn oblate gravity terms J2, J4 and the system mass. Besides, when Cassini flew by Titan at low altitude, the coefficient of atmospheric drag is also estimated. Modeling errors during Trajectory Control Maneuver are estimated by using a set of stochastic acceleration batches. Navigation for Cassini–Huygens uses radiometric tracking data from NASA's Deep Space Network (DSN) augmented by optical navigation from on-board images of planetary flybys [27,28].

3.5. MESSENGER

The Mercury Surface Space Environment, GEochemistry and Ranging (MESSENGER) orbiter was launched by NASA on August 3, 2004. It is the second mission to Mercury after Mariner 10 in 1975 and the first spacecraft to orbit Mercury. MESSENGER performed several successful gravity assists, including one Earth flybys, two Venus flybys, and three Mercury flybys, and entered into the orbit around Mercury finally. Each flyby changed the spacecraft's orbit orientation, inclination and size until the onboard propellant is able to attain the orbit around Mercury. The navigation measurements were provided by the Earth-based radio system of DSN, and Mercury Dual Imaging System (MDIS) on-board [29]. During the Earth flyby and the two Venus flybys, images of Earth, Moon and Venus were acquired with MDIS to test optical navigation in order to ensure the Mercury flyby in January 2008 [30–33]. Radiometric data, optical image of landmarks, and laser altimeter data will also be used during the Mercury orbit phase to enhance navigation performance. 10 km uncertainty is obtained before the Mercury encounter in the *B*-plane [34,35].

3.6. Rosetta

Rosetta was launched on March 2, 2004 by ESA to study the comet 67P/Churyumov–Gerasimenko for unlocking the secrets of how the solar system looked before the planets formed. Rosetta experiences four planetary swingbys, three at Earth, one at Mars to approach the comet. Two asteroid flybys are contained, one at asteroid 2867 Stein, the second at 21 Lutetia. In addition to radiometric data, pictures of asteroid against the background stars taken by two on-board navigation cameras (NAVCAM) and Optical, Spectroscopic, and Infrared Remote Imaging System (OSIRIS) are used to navigate Rosetta autonomously towards the asteroid. The optical measurement reached an accuracy of 0.1 pixels, a square root information filter is used, and eventually results in 2.6 km off its nominal value in the *B*-plane. Rosetta is the first mission for ESA to navigate a spacecraft using the autonomous navigation based on optical images and radiometric data [36–39]. Optical navigation is also considered as a foreseen possibility to support the Mars swing-by, which, augmented with radiometric data, observes the Mars Limb and the Martian Moons. However, because of the poor geometric and the illumination condition in the actual mission, the optical navigation system took pictures before gravity assist only for gaining experience [40].

3.7. New Horizon

New Horizon was launched on January 19, 2006 by NASA to the dwarf planet Pluto. Pluto and its moons, Charon, Nix, and Hydra, are intended to be studied, and so are the Kuiper belt objects. After New Horizon received a Jupiter gravity assist in February 2007, it changed its direction and was boosted to Pluto. It will arrive at Pluto in the summer of 2015. Combined with radiometric data, optical pictures of Pluto and Charon captured by Long Range Reconnaissance Imager (LORRI) and Multispectral Visible Imaging Camera (MVIC) will be used to achieve the accurate orbit determination during the encounter. The square root information filter will be also be used to estimate the orbit, and the best estimation will be mapped to the Pluto *B*-plane. An accuracy of less than 10 km is expected to be achieved [41,42].

3.8. Dawn

NASA launched Dawn Spacecraft on September 27, 2007. The scientific goal of Dawn is to study the conditions and processes of the solar system's earliest epoch by visiting both the asteroid Vesta and dwarf planet Ceres. Dawn used Mars's gravity to accelerate it to the main asteroid belt in February 2009. In the Mars approach phase, a Visible and Infrared Spectrometer (VIS) and two Framing Cameras imaged the Mars for calibration. When Dawn encounters a steroid, optical pictures obtained by two Framing Cameras are augmented to radiometric data to determine the orbit of the spacecraft, the ephemeris and the gravity of the asteroid, etc [44–47].

3.9. BepiColombo

BepiColombo is a joint mission between ESA and the Japan Aerospace Exploration Agency (JAXA), and it will set off on August 15, 2015 for exploration of Mercury. The mission includes two spacecraft: the Mercury Planetary Orbiter (MPO) and the Mercury Magnetospheric Orbiter (MMO). The BepiColombo will experience a 6-year interplanetary cruise through gravity assists from the Moon, Earth, Venus and arrive at Mercury eventually. Since the autonomous navigation technology of ESA is mature enough, the optical navigation system will be considered as a regular payload for interplanetary missions. The MPO will carry an imaging system consisting of a wide-angle and narrow angle camera, which is able to provide capability for MPO to navigate itself in planet approach phase, including gravity-assist phases.

3.10. OSIRIS-Rex

OSIRIS-Rex will be launched in 2016 by NASA. It is intended to visit the near-Earth asteroid 1999 RQ36, and carry samples from the asteroid back to Earth. The OSIRIS-REx Camera Suite (OCAMS) consists of the PolyCam, the MapCam, and the SamCam. PolyCam is a telescope to acquire the asteroid at long range and image it at high resolution from closer ranges. MapCam informs the model of asteroid shape and obtains high resolution imaging of the sample-set. SamCam continuously records the sample acquisitions. Each imager is backed up by one of the other two imagers, which is able to perform imaging to verify the spacecraft/1999 RQ36 relative velocity, the essential part of autonomous navigation.

Table 1 shows several successful applications of autonomous navigation in gravity-assist interplanetary missions [15–61]. Table 1 shows that autonomous navigation technology has been successfully implemented in the past gravity-assist interplanetary missions, such as Mariner 10, Voyager, and Galileo, etc. In the future, gravity assist technique will be designed in most of the interplanetary missions, and the spacecraft of those missions installs the imaging payload for autonomous navigation. Hence, the autonomous navigation is an important technology which provides superior navigation results and guarantees the success of the interplanetary mission using gravity assist. NASA, ESA, and ISAS have investigated the autonomous navigation technology for a long time, and China will pay particular attention to the autonomous navigation technology for interplanetary missions using gravity assist.

4. Key-point technology of autonomous navigation for gravity-assist spacecraft

4.1. Navigation scheme

After several gravity-assist interplanetary missions are analyzed in Section 3, three major navigation schemes for gravity assist spacecraft are presented as follows.

4.1.1. Navigations by observing beacons in distance during the cruise phase

All the bodies of the solar system are potential candidates, including planets, satellites, asteroids and comets. The most practical beacons are asteroids and planets. Planets are the brightest bodies in our solar system except the sun, which means the planets are easy to be observed. Additionally, in the solar system, there are numerous asteroids between the orbits of Mars and Jupiter, which provide sufficient navigation references.

Gravity-assist interplanetary missions, such as SMART-1 [60], have successfully utilized this navigation scheme for the cruise phase. Although this navigation scheme is not as accurate as radiometric navigation, it provides almost spherical navigation information whereas the radiometric one always has some inobservability in the Earth-probe direction.

4.1.2. Navigations by observing planets, and their natural satellites during the approach phase

Assisted-planet, destination planet, and their natural satellites are close to the spacecraft during the approach phase, which facilitates the observations. The observations are capable of providing the spacecraft with precise position and velocity with respect to the observed objects.

This navigation scheme is able to validate the autonomous navigation technology when the spacecraft is close to the Earth. MESSENGER [32] and Dawn [44] are two typical examples. When they encounter Earth, pictures of the encounter celestial body and its satellites (Moon) are taken by the on-board navigation camera. With the aid of those pictures, navigation results are provided by the autonomous navigation system on-board. By comparing that with the results created by Deep Space Network (DSN), the performance of the autonomous navigation system on-board is tested and verified. Also, in-flight calibration of the on-board navigation camera is completed after that, which guarantees the accuracy of the autonomous navigation in further phases. When the spacecraft comes across the assisted-planet, or destination planet, this navigation scheme finally achieves its capability of determining the relative position and velocity of the spacecraft to ensure the precise orbit insertion and swing by.

4.1.3. Navigations by integrated optical measurement and radio measurement

Spacecraft communicates with DSN by radio measurement, Doppler range signals, in order to determine the position and velocity of the spacecraft in relation to the Earth, which provides sufficient navigation accuracy to the earth. However, it can hardly satisfy the accuracy and real-time requirements during the gravity

Table 1
Applications of autonomous navigation in gravity-assist interplanetary missions.

Num.	Launch Time	Mission	Nation	Autonomous navigation	Sensor	Assisted planet
1.	1972.3.2	Pioneer 10 (spin-stabilized)	NASA	N.A.	N.A.	Jupiter
2.	1973.4.6	Pioneer 11 (spin-stabilized)	NASA	N.A.	N.A.	Jupiter
3.	1973.11.3	Mariner 10 (three axis stabilized)	NASA	**Phase:** approach. **Measurement:** radiometric data and optical data (Mercury and background stars). **Filter method:** least square batch filter and sequential filter and smoother.	TV Camera A and B	Venus
4.	1977.8.20	Voyager II (three axis stabilized)	NASA/JPL	**Phase:** approach. **Measurement:** radiometric data and optical data (Moons of satellite and background stars). **Filter method:** least square batch filter and sequential filter and smoother.	Imaging NA/WA	Saturn Jupiter Uranus Neptune
5.	1977.9.5	Voyager I (three axis stabilized)	NASA/JPL	The Same as Voyager II.	Imaging NA/WA	Saturn, Jupiter
6.	1989.10.18	Galileo (three axis stabilized)	NASA	**Phase:** approach (Asteroid/Jupiter) **Measurement:** radiometric data and Optical data (asteroids and stars, Galilean moons and stars). **Filter:** sequential filtering method. **Accuracy:**20 km.	SSI	1 Venus 2 Earth
7.	1990.10.6	Ulysses (spin-stabilized)	NASA/ESA	N.A.	N.A.	Jupiter
8.	1990.1.24	Muses-A (Hiten) (spin-stabilized)	ISAS	**Measurement:** radiometric data, optical data (Moon/Sun/Planet/Star). **Filter:** Least-square filter. **Accuracy:** a few km < 10. **Achievement:** world's first optical navigation system for a spin-stabilizing satellite.	ONS and SHCI	10 Moon
9.	1996.2.17	NEAR (three axis stabilized)	NASA/APL	**Phase:** approach (Earth/Eros) **Measurement**: radiometric data and optical data (Earth/Moon/Eros). **Filter Method:** square root information filter.	Multispectral Imager	Earth 1998.1.23
10.	1997.10.6 (In progress)	Cassini (three axis stabilized)	NASA/ESA/ASI	**Phase:** approach (Saturn/Titan). **Measurement:** radiometric data and optical data (satellites of Saturn). **Filter:** pseudo-epoch state estimation filter. **Accuracy:** 12 km.	ISS (Imaging Science Subsystem)	2 Venus 1 Earth 1 Jupiter 60 Saturn 33 Titan
11.	1999.2.7	Stardust (three axis stabilized)	NASA/JPL	**Phase:** approach (Earth/Wild-2/Tempel1) **Measurement:** 2-way Doppler/Range data and optical data (stars and comet). **Filter:** a square root information (SRIF) weighted least squares filter. **Accuracy:** 6 km.	Navigation Camera	Earth
12.	2003.9.27	SMART-1 (three axis stabilized)	ESA	**Phase:** cruise (Moon) **Measurement:** optical data (Moon/Earth/Asteroid). **Filter:** a square root information filter. **Accuracy:** 230 km.	AMIE	2 Moon
13.	2004.8.3 (In progress)	MESSENGER (three axis stabilized)	NASA	**Phase:** approach (Earth/Venus/Mercury), Orbit (Mercury). **Measurement:** radiometric data, optical data (Earth–Moon/Venus/Mercury), laser altimeter data (orbiting). **Filter Method:** batch Filter/Kalman Filter. **Accuracy:** < 10 km.	MDIS (WAC/NAC)	1 Earth 2 Venus 3 Mercury
14.	2004.3.2 (In progress)	Rosetta (three axis stabilized)	ESA	**Phase:** approach (Stein, Lutetia), flyby (Stein, Lutetia)	NAVCAM OSIRIS	3 Earth 1 Mars

Table 1 (*continued*)

Num.	Launch Time	Mission	Nation	Autonomous navigation	Sensor	Assisted planet
				Measurement: radiometric data, optical data. **Filter:** a square root information filter. **Accuracy:** 20 km (asteroid).	(NAC/WAC)	
15.	2006.1.19 (In progress)	New Horizons (three axis stabilized)	NASA	**Phase:** approach (Pluto) **Measurement:** radiometric data, optical data (Pluto.Charon) **Filter:** square root information filter. **Accuracy:** < 10 km.	LORRI (5 urad) MVIC Camera (20 urad)	Jupiter
16.	2006.10. 26	STEREO (A/B) (three axis stabilized)	NASA/JHU/APL	N.A.	SECCHI	Moon
17.	2007.9.27 (In progress)	Dawn (three axis stabilized)	NASA	**Phase:** approach (asteroid) **Measurement:** radiometric data, optical data (landmarks) **Filter:** a square root information weighted least squares filter. **Accuracy:** 1.2–0.8 km (early approach), 0.5 km (late approach).	Visible and infrared spectrometer and framing camera	Mars
18.	2014	BepiColombo (MMO/MPO) (spin-stabilized/three axis stabilized)	ESA/JAXA	N.A.	NAC/WAC	Moon Earth Venus Mercury
19.	2014	Solar Probe	NASA	N.A.	N.A.	Jupiter
20.	2015	Solar Probe Plus	NASA/JPL	N.A.	N.A.	7 Venus
21.	2016	Juno (spin-stabilized)	NASA	N.A.	JunoCam	Earth
22.	2016	OSIRIS-Rex	NASA	N.A.	OCAMS	Earth

assist or approach phase for suffering the ephemeris uncertainty. Optical navigation can obtain the high precision target-relative navigation information by means of observing the azimuth, elevation and pictures between celestial bodies. Integrated navigation can comprehensively take their advantages for obtaining the precise navigation information with respect to both the Earth and the assisted-planet (or destination planet), and is also capable of estimating and updating the planet ephemeris. Most gravity-assist interplanetary missions in the past generally adopt this navigation scheme [53,42], which is the main configuration of the navigation system for gravity-assist interplanetary missions.

4.2. Sensors

Performance of sensors plays an important role in the accuracy and reliability of the autonomous navigation system with gravity-assist mission. Table 2 shows characteristics of imaging sensors used in gravity-assist interplanetary missions. From Table 2, several features of sensors used in interplanetary missions are summarized.

4.2.1. Wide dynamic range and long exposure time

Sensors with wide dynamic range and long exposure time ensure that the picture includes both the assisted-planet and background stars, which is important for determining the pointing direction and navigation performance.

The fact that the assisted-planet and background stars are in the same picture is a matter of significance for the accuracy of autonomous navigation, which determines the spacecraft position by observing the angle between the assisted-planet and stars. Combining background stars and the assisted-planet, the angle between them can be directly provided, the accuracy of which is only associated with the measuring accuracy, and can offer a superior accuracy. Without the background stars, the star tracker is necessary for determining the pointing direction of the optical axis. Several complicated steps have to be carried out, including determining the vector of the stars in star tracker, obtaining the inertial attitude of the spacecraft, and giving the assisted-planet inertial vector. Through the computation, the errors involving the star tracker alignment and the sensor alignment are accumulated, which degrade the accuracy of the autonomous navigation.

Wide dynamic range and long exposure time are essential for picturing the assisted-planet and background stars simultaneously. Background stars are much dimmer than the assisted-planet, and in the absence of the wide dynamic range and long exposure time, the sensor is only able to picture the assisted-planet except the dim background stars. Therefore, wide dynamic range and long exposure time are two important criteria for sensors.

4.2.2. Dedicated navigation sensors and scientific imaging payload for redundancy

Scientific payloads on gravity assist spacecraft usually include imaging sensors, such as Optical, Spectroscopic and Infrared Remote Imaging System (OSIRIS) in the Rosetta mission [36]. Imaging is the most common function performed by both scientific payload and dedicated navigation sensors, which provide redundancy for each other. Although a scientific imaging payload is more inaccurate and inefficient than the navigation sensor, it can picture the assisted-planet and background stars for navigation when the navigation sensor is not available. The redundancy configuration achieves on-board autonomous navigation and has successfully maintained the safety of the spacecraft.

Table 2
Characteristics of sensors on deep space spacecraft using gravity assist.

Sensors in missions	Focal length	Field of view	Frame	Exposure time	Resolution	Dynamic range	Focal ratio
Mariner10 TV camera [48]	150 cm	0.37° × 0.48°	700 × 832	3 ms–12 s	9.1 × 9.9 mrad	256:1	*f*/8.43
NEAR Multispectral Imager [24]	167.35 mm	2.93° × 2.25°	537 × 244	1–999 ms	96 × 162 mrad/ pixel	2048:1	*f*/3.44
Cassini NAC [28]	2000 mm	0.35° × 0.35°	1024 × 1024	5 ms–1200 s	6 μrad/pixel	4096:1	*f*/10.5
Stardust Navigation Camera [56]	200 mm	3.5° × 3.5°	1024 × 1024	5 ms–20 s	50 μrad/pixel	4096:1	*f*/3.5
Smart-1 AMIE [60]	154 mm	5.3° × 5.3°	1024 × 1024 CCD	10 ms–10 s	0.00576°/pixel	1024:1	*f*/10
Rosetta Navigation Camera*2 [38]	152.5 mm	5° × 5°	1024 × 1024 CCD	NA	5 md/pixel	4096:1	*f*/2.17
Rosetta OSIRIS [38]	717.4 mm/ 136 mm	2.20° × 2.22°/ 11.34° × 12.11°	2048 × 2048	10 ms–5 s	18.6 μrad/pixel, 100 μrad//pixel	65535:1	*f*/8, *f*/5.6
MESSENGER MDIS [29]	550 mm 78 mm	1.5° × 1.5° 10.5° × 10.5°	1024 × 1024	1 ms–10 s	14 mm//pixel	4096:1	*f*/18 *f*/5
Dawn Framing Camera [45]	150 mm	5.5° × 5.5°	1024 × 1024 CCD	100 ms–1 s	93.7 μrad//pixel	65535:1	*f*/7.5

4.3. Filter algorithm

Two general types of filter algorithms are used in the autonomous navigation system of the gravity-assist spacecraft: batch filter and sequential filter. The batch filter provides navigation information non-recursively at some chosen epoch using an entire batch of data (such as least squares batch filter). The sequential filter provides the optimal navigation estimates at the current time by updating the states recursively (such as Kalman filter, Extended Kalman filter, and Unscented Kalman filter) [62–64].

4.3.1. Batch filter

The batch filter has been the classic approach for most of the gravity assist missions, solving the states yielding a minimum value of the performance index as the optimal navigation estimates [49]. It is easy to carry out without knowing any prior statistic information, and in post-flight orbit determination it provides better performance than the sequential filter, such as Extended Kalman filter. However, this filter is not sufficient when the spacecraft dynamics are complicated and many parameters in the model need to be solved.

4.3.2. Sequential filter

Since real-time navigation is the foundation of the real-time control, the real-time filter processing the measurement is necessary. Compared to the least square batch filter, the sequential filter requires less storage, processes faster, which leads to wide utilization in gravity-assist mission. The sequential filter is able to account for small spacecraft forces that the batch filter was unable to handle effectively [49].

5. Trends of autonomous navigation technology for gravity assist spacecraft

5.1. Optical navigation trends

In principle, optical navigation is based on the geometry method to determine the position of the spacecraft. Compared with the other autonomous navigation method, optical navigation technology has made great progress and been successfully applied in interplanetary missions [65].

Future gravity-assist interplanetary missions require both the high precision location performance and the capability of determining the surface, shape, gravity of the celestial body to improve the performance of the autonomous navigation system [66].

The terrain and the shape of the celestial body provide plenty of navigation information for the spacecraft during the swing-by, which is obtained at close range and remotely, respectively. In order to obtain the landmark and the limb, two kinds of cameras, both wide and narrow angles, need to be utilized in navigation system. Narrow Angle Camera (NAC) images distant pictures during the cruise phase and the early phase of the rendezvous. The Wide Angle Camera (WAC) takes the picture at short range for the gravity-assist phase (approach phase), descent phase, and middle and last phase of the rendezvous. The technology of image process used in NAC and WAC is different. The center finding process is carried on for the small image of a celestial body in NAC picture, whereas terrain recognition and targeting of the image area are used for the image of the celestial body area in WAC camera. Therefore, the integration of two cameras is beneficial for high precision navigation in all phases.

In addition, a gimbal can be implemented on the sensor in the future, which would avoid the need to slay the whole spacecraft in order to take pictures. The gimbal-mounted sensor is capable of observing different celestial bodies eliminating the need for turning the spacecraft, and obtaining pictures of the same area such as targeting the landmark [67].

5.2. X-ray navigation trends

Navigation using X-ray pulsar is a new generation of autonomous navigation to give the position of the spacecraft by indirectly calculating the difference between the measured time of arrivals and the best pulsar-timing model. Compared to optical navigation, the higher frequency of X-ray pulsars leads to more precise navigation results. Therefore X-ray pulsar is a potential and important navigation method in future gravity-assist missions.

At present, candidates for X-ray pulsars navigation are limited. With long observation time of X-ray pulsars in the sky on Earth, more pulsars could be used in interplanetary navigation. In terms of geometric distributions, characteristics and achievable accuracies, the selection of X-ray pulsars for higher precision navigation performance is a hot spot in future investigations.

To enhance the observing accuracy of X-ray pulsar photon time of arrivals (TOA), error sources influence on navigation performance needs to be analyzed and handled appropriately, including detector errors, measurement errors, source model errors, spacecraft system errors, etc [68–70]. Besides, the technologies involved with processing pulsar profile are also of interest to investigate in future, including period ambiguity problem, fast signal processing, Doppler effect, phase delay, etc.

An accurate model of the pulsar observation can provide precise location performance for the spacecraft. However, the accurate observation model is usually nonlinear, which requires

the nonlinear filtering method used in X-ray pulsar navigation of interplanetary missions [71].

5.3. Optical Doppler navigation trends

An optical Doppler navigation system measures Doppler shift frequency spectra (such as red shift or blue shift in astronomy) to determine the velocity of the spacecraft, and give the continuous position indirectly by integration [72,73,74]. At least three optical objects should be observed to obtain the velocity vector of the spacecraft. If only one or two objects can be observed, the orbital dynamics and Kalman filter should be involved. By optical Doppler measurement, the velocity can be directly measured, and therefore a continuous position can be provided. Those advantages of optical Doppler navigation methods overcome the shortcomings of the other position-based navigation methods, such as long-time observation. Thus as the complement of the other position-based navigation method, it is a potential navigation method in future gravity-assist missions.

However, as a novel autonomous navigation method, optical doppler navigation system is not ready for the application of deep space missions. Therefore, for successful applications of maser-based navigation in interplanetary missions, it is necessary to make a breakthrough in on-board sensor (optical spectrometer), selection of maser candidate, study of maser source characteristics, accurate measurement model, and error budget, etc.

5.4. Inertial navigation trends

For the state-of-the-art accuracy of inertial instruments, inertial navigation is mainly utilized in the attitude determination system of interplanetary spacecraft. However, because of the poor sensitivity of non-gravity force acting on the spacecraft, inertial navigation can only be used in the terminal approach phase to measure the orbit insertion maneuver, and Enter, Descent, Landing (EDL) phase to measure the gravity acceleration [75]. With the rapid development of modern physics, such as quantum mechanics, atomic manipulation and modern optics, the cold-atom interferometer accelerometer using atomic manipulation technologies has been a focus of attention, aiming to achieve ultra-high precision acceleration [76,77]. As a result, the complicated dynamical perturbations are able to be modeled and compensated by this novel ultra-high precision measurement. In addition, the novel accelerometer could be useful to explain the fly-by anomalies encountered by a number of gravity-assist spacecrafts [78].

5.5. Integrated navigation trends

Several types of navigation methods are used in gravity assist mission: radio navigation, optical navigation, inertial navigation, etc. Radio navigation measurement, Range-Doppler, provides the accurate position and velocity of the spacecraft with respect to the Earth. However, this option cannot guarantee the necessary approach accuracy for an interplanetary mission when the ephemeris uncertainty of the destination body is hardly ignored. Additionally, its communication performance, such as real-time performance and coverage performance, limits its application. Although optical navigation measurement is less accurate than radio measurement, it is directed with respect to the destination body, which offers superior navigation performance near the destination body. Inertial navigation uses force models to propagate position and velocity by sensing the non-gravitational force acting on the spacecraft with accelerometers (perhaps cold-atom interferometers accelerometers in the future). Its accuracy degrades for long-term solution by the nonmodeled perturbations. Considering the advantage and disadvantage of three methods, integrated navigation is a realistic path for high precision navigation performance, which can calibrate the ephemeris uncertainty, compensate the perturbations, and satisfy the requirements of accuracy, autonomy and reliability eventually [65,71].

5.6. Inter-Sat communication navigation trends

Three Inter-Sat navigation methods are expected to be utilized in interplanetary missions: (1) Satellite-to-Satellite radiometric tracking; (2) optical observation of other satellites; and (3) quantum positioning. All three Inter-Sat navigation methods provide gravity-assist missions with more available options and redundancy, when more than two independent methods of autonomous navigation are used, including methods used in single satellite and those used in multisatellite.

5.6.1. Satellite-to-Satellite radiometric tracking

One Satellite-to-Satellite radiometric tracking method obtains relative navigation information of two or more satellites whose absolute position is known. This method is currently used in Mars Explorations. Taking Mars Science Laboratory (MSL) as an illustration, MRO and Odyssey spacecraft serve as beacons and help orbit determination of MSL via radio signals of Ultra High Frequencies (UHF). A Mars Network based on Satellite-to-Satellite radiometric tracking has been used for Mars exploration mission [79]. It is designed to aid Mars Approach, Entry/Descent/Landing (EDL) navigation, and considering the similarity between approach phase and gravity-assist phase, the Mars network can be potentially used in future gravity-assist missions.

Another Satellite-to-Satellite tracking (SST) method, called linked, autonomous, interplanetary satellite orbit navigation (LIAISON), determines the relative and absolute orbits of two or more spacecrafts. This method requires that at least one of the satellites is in an orbit with a unique size, shape and orientation, such as spacecraft in halo orbit or at Sun–Earth L_1 and L_2 [80,81]. The merit of this method is that the relative and absolute orbit states for all participating spacecrafts can be well estimated simultaneously. This concept has not been successfully used in actual missions, and the real data obtained from a halo orbiter can be used as validation and evaluated the navigation performance, and extend its results to other possible missions, including a gravity-assist spacecraft. As more spacecrafts will be launched at libration point in the coming year, it is believed that this method will be available in the near future, and provides navigation support for various kinds of interplanetary missions.

5.6.2. Optical observation of other satellites

Optical observations of other spacecrafts are a suggested method for orbit determination. The Lunar Lander Altair of Project Constellation was planned to take the star-like images of geostationary or MEO communications and navigation satellites in the Earth–Moon cruise for the purpose of navigation [65]. This method is similar to the first one of SST method because both of them provide the relative motion information, and require the accurate absolute position of the observation satellite. This method can be also used in gravity-assist missions or approaching phase of interplanetary missions, when the gravity-assist target is surrounded by other satellites, the orbit of which is well determined.

5.6.3. Quantum positioning

Positioning using entangled–squeezed quantum is a novel concept. Thomas B. Bahder proposed a quantum positioning system (QPS) that uses three interferometers (which generate entangled photon pairs) together to solve for the spatial position

and an additional interferometer to solve for the time. The navigation principle is similar to Global Positioning System and X-ray pulsar system. The merit of this method is that four of the space-time coordinates are able to be provided. Also, using quantum as asignal, instead of using microwaveswave, breaks the limit of the power and the bandwidth, and precision information can be extracted from the faint quantum signal. However, it has to experience a long-term developing period to break through core technologies to equip spacecraft with quantum navigation system and extend its application to deep space [82,83].

6. Conclusions

After the successful Lunar Exploration Mission Program, China is going to fulfill a Deep Space Exploration Program to explore Mars, Venus, the solar system and beyond in the future. Gravity assist technique can provide considerable supports for the interplanetary transfer; as a result, the autonomous navigation technology, as one of the primary navigation methods, is paid more attention to. Theories and methods of autonomous navigation are beneficial for designing guidance, navigation, and control system of the deep space missions using gravity assist.

Acknowledgments

The work described in the current paper was supported by the National Natural Science Foundation of China (Nos. 61233005 and 61004140), the National Defense Basic Research Program, the New Century Program for Excellent Talents of the Ministry of Education of China, National Basic Research Program of China (No.2014CB744200), Scholarship for Short-Term Study Abroad, and the Astronautics Science and Technology Innovation Fund. The authors would like to thank all members of Science and Technology on Inertial Laboratory and Fundamental Science on Novel Inertial Instrument and Navigation System Technology Laboratory for their useful comments regarding this work.

References

[1] Wu Weiren, Liu Wangwang, Qiao Dong, Jie Degang. Investigation on the development of deep space exploration. Science China: Technological Sciences 2012;55(4):1086–1091.
[2] Weiren Wu, Dayi Wang, Xiaolin Ning. Principle and technology of autonomous navigation for deep space probe. Beijing, China: Astronautic Publishing House; 2011.
[3] Jiancheng Fang, Xiaolin Ning. Methods of autonomous celestial navigation for deep space probe. Xi'an: Northwestern Polytechnical University Press; 2010.
[4] Dayi Wang, Xiangyu Huang, Chunling Wei. Principle and technology of autonomous control based on optical image measurement for deep space probe. Beijing, China: Astronautic Publishing House; 2012.
[5] Chobotov VA. Orbital mechanics. 3rd ed. New York: Oxford University Press; 2002.
[6] Lohar FA, Misra AK, Mateescu D. Mars–Jupiter aerogravity assist trajectories for high-energy missions. Journal of Spacecraft and Rockets 1997;34(1):16–21.
[7] Rourke KH, Acton CH, Breckenridge WG, Campbell JK, Christensen CS, Donegan AJ. The determination of the interplanetary orbits of Vikings 1 and 2. In: Proceedings of the AIAA the15th aerospace sciences meeting; 1977. p. 1–23.
[8] Kizner W. A method of describing miss distance for lunar and interplanetary trajectories. Planetary and Space Science 1961;7(7):125–131.
[9] Jiachi Yang. Spacecraft orbit mechanics and control. Beijing, China: Astronautic Publishing House; 2011.
[10] Riedel JE, Bhaskara S, Desai S, Han D, Kennedy B, Null GW. Autonomous optical navigation DS1 technology validation report. California, USA: Jet Propulsion Laboratory (JPL Publication 00-10); 2000.
[11] Mancuso S. Vision based GNC systems for planetary exploration. In: Proceedings of the 6th conference on dynamics and control of systems and structures in space; 2004.
[12] Martin-Mur TJ, Bhaskaran S, Cesarone RJ, McElrath T. The next 25 years of deep space navigation. In: Proceedings of the 2008 AAS guidance navigation and control conference; 2008.
[13] Duxbury TC, Born GH, Jerath N. Viewing Phobos and Deimos for navigating Mariner 9. Journal of Spacecraft and Rockets 1974;11(4):215–222.
[14] Jun'ichiro Kawaguchi, Tatsuaki Hashimoto, Ichiro Nakatani, Keiken Ninomiya. On autonomous imagery of Phobos and Deimos using flyby camera on board Planet-B spacecraft. In: Proceedings of the AIAA guidance, navigation and control conference; 1993. p. 483–91.
[15] Kechichian JA, Kenyon PR, Moultrie B. Orbit determination accuracy assessment for an asteroid flyby: a Galileo case study. In: Proceedings of the AIAA 25th aerospace sciences meeting; 1987. p. 1–12.
[16] Kallemeyn PH, Haw RJ, Pollmeier VM, Nicholson FT. Galileo orbit determination for the Gaspra asteroid encounter. In: Proceedings of the 1992 AIAA/AAS astrodynamics conference; 1992. p. 370–80.
[17] Miller LJ, Miller JK, Kirhofer WE. Navigation of the Galileo mission. In: Proceedings of the AIAA the 21st aerospace sciences meeting; 1983. p. 1–19.
[18] Kenyon PR, Kechichian JA. Galileo probe delivery and orbit approach orbit determination. In: Proceedings of the AIAA the 25th aerospace sciences meeting; 1987. p. 1–11.
[19] Kawaguchi Junichiro, Yamada Takahiro, Hashimoto Tatsuaki, Sawai Shujiro, Ninomiya Keiken. On the operation of lunar and interplanetary spacecraft at ISAS. Acta Astronautica 1995;37:141–151.
[20] Uesugi K. Results of the MUSES-A HITEN mission. Advances in Space Research 1996;18(11):69–72.
[21] Nishimura T, Ninomiya K, Ichikawa T, Noguchi K, Namera T. Experimental optical navigation and guidance for Muses-A. In: Proceedings of the 39th international astronautical congress; 1988. p. 1–9.
[22] Nishimura Toshimitsu, Ichikawa Tsutomu, Ushikoshi Atsuo, Kosaka Hiroshi. Tracking of MUSES-A 'Hiten' and description of software package ISSOP for orbit determination. Japanese Institute of Space and Astronautical Science technical report (no. 70) 1991-03.1991.
[23] Owen WM, Wang TC. NEAR optical navigation at Eros. NASA Report 01-1429.2001.
[24] Hawkins SE. Overview of the multi-spcetral imager on the NEAR spacecraft. Acta Astronautica 1997;39(1–4):265–271.
[25] Prockter L, Murchie S, Cheng A, Krimigis S, Farquhar R, Santo A. The NEAR Shoemaker mission to asteroid 433 Eros. Acta Astronautica 2002;51(1–9):491–5500.
[26] Williams BG, Miller JK, Antreasian PG, Helfrich CE, Owen WM, Yeomans DK. Challenges in NEAR Navigation. JPL Technical Report 99-1820.1999.
[27] Antreasian PG, Ardalan SM, Beswick RM. Orbit determination processes for the navigation of the Cassini–Huygens mission. In: Proceedings of the SpaceOps 2008 Conference; 2008.
[28] Jaffe LD, Herrell LM. Cassini/Huygens science instruments, spacecraft, and mission. Journal of Spacecraft and Rockets 1997;34(4):509–521.
[29] Hawkins SE, Boldt JD, Darlington EH, Espiritu R, Gold RE, Gotwols B. The Mercury dual imaging system on the MESSENGER spacecraft. Space Science Reviews 2007;131(1–4):247–338.
[30] Holdridge ME, Calloway AB. Launch and early operation of the MESSENGER mission. Space Science Reviews 2007;131(1–4):573–600.
[31] Vaughan RM, Leary JC, Conde RF. Return to Mercury: the MESSENGER spacecraft and mission. In: Proceedings of the 2006 IEEE aerospace conference; 2006. p. 1–16.
[32] McNutt Jr. RL, Solomon SC, Grant DG. The MESSENGER mission to Mercury: status after the Venus flybys. Acta Astronautica 2008;63(1–4):68–73.
[33] Artis DA, Heggestad BK, Krupiarz CJ, Mirantes MA, Reid JD. MESSENGER: flight software design for a deep space mission. In: Proceedings of the 2007 IEEE aerospace conference; 2007. p. 1–9.
[34] Williams B, Taylor A, Carranza E, Miller J, Stanbridge D, Page B. Early navigation results for NASA's MESSENGER mission to Mercury. In: Proceedings of the 15th AAS/AIAA space flight mechanics conference; 2005. p. 1–18.
[35] Solomon SC, McNutt RL, Gold RE. MESSENGER mission overview. Space Science Reviews 2007;131:3–39.
[36] Thomas N, Keller HU, Arijs E. OSIRIS—the optical spectroscopic, and infrared remote imaging system for the Rosetta orbiter. Advances in Space Research 1998;21(11):1505–1515.
[37] Da DV, Naletto G, Nicolosi G, Zambolin P, Pelizzo M. Optical performances of the wide angle camera for the Rosetta mission: preliminary results. In: Proceedings of the SPIE; 2001.
[38] Mathias Lauer, Ulrich Herfort, Dave Hocken, Sabine Kielbassa. Optical measurements for the flyby navigation of Rosetta at asteroid Steins. In: Proceedings of the 21st international symposium on space flight dynamics; 2009. p. 1–15.
[39] Hechler Mclrtin. Rosetta mission design. Advances in Space Research 1997;19(1):127–136.
[40] Frank Budnik, Trevor Morley. Rosetta navigation at its Mars swing-by. In: Proceedings of the international symposium on space technology and science, vol. 25; 2006. p. 593.
[41] Weaver HA, Gibson WC, Tapley MB, Young LA, Stern SA. Overview of the New Horizons science payload. Space Science Reviews 2008;140(1–4):75–91.
[42] Reuter D, Stern S, Scherrer J, Jennings D, Baer J, Hanley J, et al. Ralph: a visible/infrared imager for the New Horizons Pluto/Kuiper belt mission. Space Science Reviews 2008;140(1–4):129–154.
[43] Miller JK, Stanbrdge DR, William BG. New Horizons Pluto approach navigation. AAS Report (AAS 04-136).2004.
[44] Russell CT, Coradini A, Christensen U, De Sanctis MC, Feldman WC, Jaumann R. Dawn: a journey in space and time. Planetary and Space Science 2004;52:465–489.

[45] Sierks H, Keller HU, Jaumann R, Michalik H, Behnke T, Bubenhagen F. The Dawn framing camera. Space Science Reviews 2011;163(1–4):263–327.
[46] Mastrodemos N, Rush B, Vaughan D, Owen B. Optical navigation for Dawn at Vesta. In: Proceedings of the 21st AAS/AIAA space flight mechanics meetings; 2011.
[47] Konopliv AS, Asmar SW, Bills BG. The Dawn gravity investigation at Vesta and Ceres. Space Science Reviews 2011;163:461–486.
[48] Stanton RH, Ohtakay H, Miller JA, Voge CC. Demonstration of optical navigation measurements on Mariner 10. In: Proceedings of the AIAA the 13th aerospace sciences meeting; 1975. p. 1–11.
[49] Christensen CS, Reinbold SJ. Navigation of the Mariner10 spacecraft to Venus and Mercury. In: Proceedings of the AIAA mechanics and control of flight conference; 1974. p. 1–8.
[50] Jacobson RA. Pioneer and Voyager Jupiter encounter orbit reconstruction in the ICRF system. In: Proceedings of the AAS/AIAA space flight mechanics meeting; 2002. p. 1–3.
[51] Campbell J, Synnott S, Bierman G. Voyager orbit determination at Jupiter. IEEE Transactions on Automatic Control 1983;28(3):256–268.
[52] Synnott SP, Donegan AJ, Riedel JE, Stuve J. Interplanetary optical navigation Voyager Uranus encounter. In: Proceedings of the AIAA 1986 astrodynamics conference; 1986. p. 192–206.
[53] Riedel JE, Owen WM, Stuve JA. Optical navigation during the Voyager Neptune encounter. In: Proceeding of the AIAA/AAS astrodynamics conference; 1990. p. 118–28.
[54] JPL News. Earth Flyby: January 15, 2001. 1100 days Since Earth Flyby [accessed 26.11.03].
[55] Menon PR. Stardust navigation covariance analysis. NASA Report 99-0508.1999.
[56] Carranza E, Kennedy B, Williams K. Orbit determination of Stardust from the Annefrank asteroid fly-by through the Wild 2 comet encounter. In: Proceedings of the 14th AAS/AIAA space flight mechanics conference; 2004.
[57] Stardust navigation camera. ⟨http://stardust.jpl.nasa.gov/mission/camera.html⟩.
[58] Marini AE, Racca GD, Foing BH. SMART-1 technology preparation for future planetary missions. Advances in Space Research 2002;30(8):1895–1900.
[59] Foing BH, Racca GD, Marini A, Evrard E, Stagnaro L, Almeida M. SMART-1 mission to the Moon: status, first results and goals. Advances in Space Research 2006;37:6–13.
[60] Pinet P, Cerroni P, Josset JL, Beauvivre S, Chevrel S, Muinonen K. The advanced Moon micro-imager experiment(AMIE) on SMART-1 scientific goals and expected results. Planetary and Space Science 2005;53(13):1309–1318.
[61] Genova A, Marabucci M, Iess L. A batch-sequential filter for the Bepicolombo Radio Science Experiment. Journal of Aerospace Engineering 2012;4(4):18.
[62] Mission overview: the giant plant story is the story of the solar system; 2009. ⟨http://www.nasa.gov/mission-pages/juno/overview/index.htm⟩ [accessed 03.03.09].
[63] Vetter JR. Fifty years of orbit determination: development of modern astrodynamics method. Johns Hopkins APL Technical Digest 2007;27(3):239–252.
[64] Vallado DA. Fundamentals of astrodynamics and applications. 3rd ed. New York: Springer-Verlag; 2007.
[65] Bhaskaran S. Autonomous navigation for deep space missions. In: Proceedings of the 12th international conference on space operations; 2012. p. 1–13.
[66] Cangahuala LA. Interplanetary navigation overview. JPL Technical Report (no. 00-1681).2000.
[67] Riedel JE, Vaughan AT, Werner RA. Optical navigation plan and strategy for the lunar lander Altair; OpNav for lunar and other crewed and robotic exploration applications. In: Proceedings of the AIAA guidance navigation and control conference; 2010. p. 1–40.
[68] Liu Jing, Ma Jie, Tian Jinwen, Kang Zhiwei, White Paul. X-ray pulsar navigation method for spacecraft with pulsar direction error. Advances in Space Research 2010;46:1409–1417.
[69] Sun Shouming, Zheng Wei, Tang Guojian. A research on the pulsar timing based on Kalman Filtering. Chinese Astronomy and Astrophysics 2010;34:187–193.
[70] Ping Shuai, Ming Li, Shaolong Chen, Huang Zhen. Principle and method of X-ray pulsar navigation system. Beijing: China Astronautic Publishing House; 2009.
[71] Emadzadeh AA, Speyer JL. Navigation in space by X-ray pulsars. New York: Spinger-Verlag; 2011.
[72] Dong J. The principle and application of maser navigation. arXiv preprint, arXiv:0901.0068; 2008.
[73] Guo Yanping. Method and apparatus for autonomous solar navigation. United States Patent: US6622970B2; 2003.
[74] Guo Y. Self-contain autonomous navigation system for deep space missions. Advances in the Astronautical Sciences 1999;102(2):1099–1113.
[75] Li Shuang, Cui Pingyuan, Cui Hutao. Vision-aided inertial navigation for pinpoint planetary landing. Aerospace Science and Technology 2007;11(6):499–506.
[76] Canuel B, Leduc F, Holleville D, Gauguet A, Fils J, Virdis A. Six-axis inertial sensor using cold-atom interferometry. Physical Review Letters 2006;97:010402.
[77] Jiancheng Fang, Jie Qin. Advances in atomic groscopes: a view from inertial navigation application. Sensors 2012;12:6331–6346.
[78] Turyshev SG, Toth VT. The puzzle of the flyby anomaly. Space Science Reviews 2009;148:169–174.
[79] Lightsey EG, Mogensen AE. Real-time navigation for Mars missions using the Mars network. Journal of Spacecraft and Rockets 2008;45(3):519–533.
[80] Hill K, Born GH. Autonomous interplanetary orbit determination using satellite-to-satellite tracking. Journal of Guidance, Control, and Dynamics 2007;30(3):679–686.
[81] Hill KA. Autonomous navigation in libration point orbits. University of Colorado; 2007 ([Doctor dissertation]).
[82] Giovannetti V, Lloyd S, Maccone L. Quantum enhanced positioning and clock synchronization. Nature 2011;412:417–419.
[83] Giovannetti V, Lloyd S, Maccone L. Positioning and clock synchronization through entanglement. Physical Review A 2002;65(2):022309.